Journal of Innovative Optical Health Sciences
Vol. 7, No. 6 (2014) 1450031 (13 pages)

DOI: 10.1142/S179354581450031X

World Scientific
www.worldscientific.com

Investigation of human visual cortex responses to flickering light using functional near infrared spectroscopy and constrained ICA

Nguyen Duc Thang*,§, Vo Van Toi*, Le Giang Tran*,
Nguyen Huynh Minh Tam† and Lan Anh Trinh‡
*Biomedical Engineering Department, International University
Vietnam National Universities HCMC, Vietnam
†University of Saskatchewan, Canada
‡Electronics Engineering Department
Posts and Telecommunications Institute of Technology
Ho Chi Minh City, Vietnam
§ndthang@hcmiu.edu.vn

Received 13 November 2013
Accepted 12 February 2014
Published 8 April 2014

The human visual sensitivity to the flickering light has been under investigation for decades. The finding of research in this area can contribute to the understanding of human visual system mechanism and visual disorders, and establishing diagnosis and treatment of diseases. The aim of this study is to investigate the effects of the flickering light to the visual cortex by monitoring the hemodynamic responses of the brain with the functional near infrared spectroscopy (fNIRS) method. Since the acquired fNIRS signals are affected by physiological factors and measurement artifacts, constrained independent component analysis (cICA) was applied to extract the actual fNIRS responses from the obtained data. The experimental results revealed significant changes ($p < 0.0001$) of the hemodynamic responses of the visual cortex from the baseline when the flickering stimulation was activated. With the uses of cICA, the contrast to noise ratio (CNR), reflecting the contrast of hemodynamic concentration between rest and task, became larger. This indicated the improvement of the fNIRS signals when the noise was eliminated. In subsequent studies, statistical analysis was used to infer the correlation between the fNIRS signals and the visual stimulus. We found that there was a slight decrease of the oxygenated hemoglobin concentration (about 5.69%) over four frequencies when the modulation increased. However, the variations of oxy and deoxy-hemoglobin were not statistically significant.

Keywords: Papillometre; visual stimulation; functional near infrared spectroscopy; constrained independent component analysis.

1. Introduction

Understanding the functioning of a visual system, from the eyes through visual cortex has progressed over centuries. Investigations to determine appropriate visual stimulations and data collection methods, and most importantly to understand the obtained responses have been widely reported in physiological and clinical research literature.[1–3]

Photic stimulation using flickering light that is modulated in sinusoidal waveform received particular attention. This is due to the fact that the stimulus parameters including modulation depth, flicker frequency and average illuminance can be adjusted at will and independently. The responses are therefore rich in information and depend only on one parameter at a time. Furthermore, the experiments can be performed *in vivo* and noninvasively. Therefore, it has been broadly applied in the studies of visual system with animal as well as human. In psychophysics, sinusoidal stimulation has been used to establish human temporal modulation transfer functions (TMTF)[4] which is the sensitivity to flickering light of various frequencies. It has a typical band-pass shape and the critical flicker frequency (CFF) which is the highest flicker frequency one can perceive is about 50 Hz. They suggested that, the blood flow in the optic nerve head is tightly coupled to neural activity. In electrophysiology, sinusoidal stimulation has been used to investigate electroretinograms (ERG), visual evoked potentials (VEP) and electrical responses of cells including photoreceptors, horizontal and ganglion cells.[5,6] These results revealed neural activities of different visual cells at different stages of the visual system. Toi and Riva[7] while investigating the retinal blood flow at the optic nerve head of cats using laser Doppler method, found that sinusoidal stimulation always caused an increase in the blood flow and the increase depended on the stimulus frequency, modulation depth and illuminance. When the modulation depth increased, the blood flow increased and, most of the time, rapidly reached a saturation level as a sigmoidal function. The TMTF was established using a minimum blood flow change as a criterion that had a band-pass shape and its high frequency slope was comparable to the slope obtained in the ganglion cell studies.[8] In functional magnetic resonance imaging (fMRI), an effective method used to measure the blood oxygen level detection (BOLD) signals, several studies revealed that the BOLD activation in the visual cortex increased when the stimulus frequency was raised up to 8 Hz.[9] Others found that BOLD activation peaked at 6–11 Hz.[10] However, fMRI is limited by its high cost and provides BOLD signals containing only deoxygenated hemoglobin information. Recently, functional near infrared spectroscopy (fNIRS) has emerged as an important modality applied to monitor the changes of oxygenated and deoxygenated hemoglobin (oxy-Hb and deoxy-Hb) concentrations. Due to its noninvasive and *in vivo* characteristics, fNIRS offers many advantages and becomes a complementary technique to fMRI. Typically, in fNIRS technology, a light within the near infrared spectrum from 700 to 900 nm wavelength is used to propagate through the brain matter. The wavelength is selected to maximize the absorption of the oxygenated and deoxygenated hemoglobin and minimize the light absorption of water and tissues. Therefore, fNIRS is able to monitor hemodynamic responses of the brain in real time.

It has been reported that fNIRS successfully monitored the hemodynamic responses at the visual cortex caused by flickering stimulation that appears on a computer screen.[11] Meek *et al.*[12] suggested that oxy-Hb concentration increased whereas deoxy-Hb concentration decreased during stimulation. Kojima and Suzuki[13] came up with similar conclusion showing typical activation patterns of hemodynamic responses during a visual task, but suggested that intense focus to stimulus led to stronger changes on oxy-Hb concentration than passive watching. The location to measure hemodynamic responses of the visual cortex was exploited by Wijeakumar *et al.*[14] Liao *et al.*[15] revealed that neurovascular coupling in and around the visual cortex appeared not only in healthy adults but also in infants during the first week of life. Bridge[16] used black and white concentric circles flickering in bulls eye with spatial frequencies grating at different temporal frequencies on the visual cortex. Experimental results showed insignificant differences of the brain responses to various temporal frequencies of stimuli.

To the best of our knowledge, there has been no investigation using fNIRS to measure the hemodynamics of the brain when the eye is stimulated by sinusoidal waveform flickering light of various

frequencies and modulations depths. When the eyes are excited by sinusoidal flickering light, neural signals are sent through optic nerve to stimulate the visual cortex. As a result, hemodynamic responses in this area may be changed and monitored by fNIRS to understand physiological and pathological principle of the ophthalmic system. This gives us useful insights on the effects of flickering light on the operations of the visual cortex and may gain benefits for the treatments of visual related diseases and disorders.

In this work, we investigated the variation of the oxy-Hb and deoxy-Hb changes at the visual cortex using fNIRS while the subjects observed a flickering light modulated sinusoidally through an eye piece under Maxwellian view.[17]

Since sensitivity of NIRS to brain activities is affected by artifacts originated from cardiac activities, Mayer waves and other physiology factors, methods to extract the actual NIRS responses from the measurement are important. Independent component analysis (ICA) constitutes a reliable method to recover source signals from mixtures and its procedure may extract task-related, physiological-related or artifact-related components. Incorporating prior constraints to ICA thereby plays an important role to isolate components targeted to specific events in event-related experiments.[18] In this work, we proposed a method using constrained ICA (cICA) to extract the NIRS signals of interest from the mixture using reference signals. After the actual NIRS signals were recovered, we varied the frequencies and modulation depth of activated light to observe the corresponding NIRS responses.

2. Methods

2.1. *Data collection protocol*

2.1.1. *Participants*

A total of 10 young and healthy subjects (age average 20.6 years old and standard deviation 0.71) of both genders (four females and six males) participated in the experiments. None of them have the neurological disorders or the visual abnormalities. The local institutional review board has approved the studies and the participants have given written informed consent for the experimental contents. The tenets of the Declaration of Helsinki were followed.

2.1.2. *Visual stimulator*

The visual stimulator Papillometre [Fig. 1(a)] has been described in details elsewhere.[17,19–21] It generates a modulated light beam. The sinusoidal waveform of the beam is expressed as follows:

$$L(t) = L_0(1 + m\cos(2\pi ft)), \tag{1}$$

where $L(t)$ is the instantaneous light intensity, L_0 the average light illuminance ranging from 0 to 100 Trolands, m the modulation depth ranging from 0 to 1 and f the flickering frequency ranging from 0 to 100 Hz. These parameters can be adjusted independently. The subject observed the stimuli under a Maxwellian view ranging from 5° to 60°. The stimulus color was white and field of view was uniform.

2.1.3. *fNIRS devices and data acquisition protocol*

Our fNIRS equipment was the FOIRE-3000 (Shimadzu, Japan) which consisted of 16 optodes (8 light sources and 8 photo detectors) and constituted a maximum of 24 channels [Fig. 1(b)]. The laser light sources have three different wavelengths 780, 805 and 830 nm.

In our experiments performed here, the transmitter and receiver optodes are arranged in a 2×3 matrix to cover the visual cortex at the back of the head [Fig. 1(c)]. The T-transmitter are symbolized by a red circle whereas the R-receiver optodes by a blue one. Each pair of T-R with a distance of 3 cm constituted a measurement channel. Together, they formed seven channels.

The subjects sat in a quiet and dark room to avoid environmental distractions [Fig. 1(d)]. Before performing the tasks, the subjects were first asked to take a rest for 40 s to release the stress and to shift their hemodynamic signals into the baseline. Then, during the next 40 s, the subject performed the task by looking through the eyepiece of the Papillometre, a visual stimulator, to observe the stimuli. The fNIRS optodes of the FOIRE 3000, fNIRS equipment, were installed on a headgear which was secured on the subject's head at the visual cortex to monitor the changes of the oxy-Hb and deoxy-Hb concentrations at this area. The task-rest experimental sequence was repeated for five times. Then, the subject will wait for several hours before he or she joins a new experimental session.

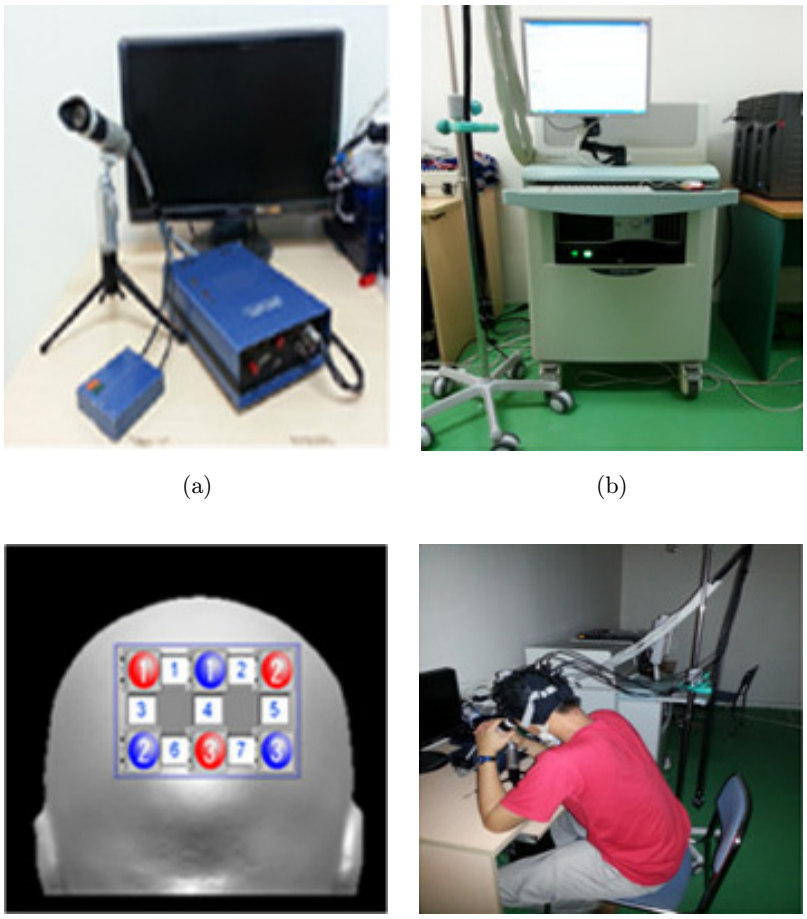

(a) (b)

(c) (d)

Fig. 1. Experimental setup. (a) Papillometre, (b) Foire-3000, (c) Location of probes and (d) Participant doing experiments.

According to reported studies,[7,10] visual stimuli with frequencies lower than 15 Hz evoked strongest visual cortex responses. Therefore, we performed the experiments using four flickering frequencies including 0, 5, 10 and 15 Hz with two modulation depths of 0.5 and 1. For each frequency and modulation depth, the experiment is repeated for two sessions. In total, each subject performed 5(epochs) × 2(sessions) × 2(modulations)× 4(frequencies) = 80 NIRS trials.

2.2. *Data processing*

Since the optodes were arranged on the subjects' scalp and the limited distance that the light can travel deep into the brain matter was about 3 cm,[22] the obtained signals were the combination of the fNIRS signals and other artifacts such as Mayer waves, heartbeat and respiration movements and physiological signals appeared at the skin of the head.

To remove a part of noises, obtained NIRS signals are filtered by low-pass and high-pass filters with the cutoff frequency of 0.5 and 0.01 Hz. Previously correlation based signal improvement (CBSI) method[23] enhanced hemodynamic responses by an assumption of strong negative correlation between oxy-Hb and deoxy-Hb signals. Typically, when oxy-Hb concentration increases, the trends of deoxy-Hb concentration goes down accordingly. Let x_0 and y_0 be the measured fNIRS signals, then true fNIRS signals are recovered by CBSI using the following equation.

$$x = \frac{1}{2}(x_0 - \alpha y_0), \qquad y = -\frac{x_0}{\alpha}, \tag{2}$$

where $\alpha = \frac{std(x_0)}{std(y_0)}$ is the ratio between the standard deviation of x_0 and of y_0. Because the NIRS measurement is performed with the probes secured at the head skin, obtained signals are the mixtures of different source signals emitted from active regions of the brain. Therefore, CBSI may magnify noninterest signals not involved to event-related paradigm in experiments.

Currently, it has been accepted that ICA presents a reliable method to separate spatially independent source signals from the mixtures. However, ICA does not concern any paradigm information to extract independent components (ICs). Therefore, in this work, we utilize a method of using cICA to better extract ICs of interest from mixtures using prior information of task-related experiments. The details of ICA and cICA are described in the following sections.

2.2.1. *Independent component analysis*

In general, blind source separation (BSS) is applied to recover original source signals from mixtures. Assuming that the measured signals are presented as $\mathbf{x}(t) = (x_1(t), x_2(t), \ldots, x_n(t))^T$ and the original signals as $\mathbf{s}(t) = (s_1(t), s_2(t), \ldots, s_m(t))^T$, ICA addresses the BSS problem in a particular situation in which $\mathbf{x}$ is a linear mixture of the sources,

$$\mathbf{x}(t) = \mathbf{A}\mathbf{s}(t), \tag{3}$$

where $\mathbf{A}$ is the mixing matrix with size $(n \times m)$. The ICA algorithm aims at computing a $(m \times n)$ demixing matrix $\mathbf{W} = [w_1, w_2, \ldots, w_m]^T$ to recover all ICs from the measurements

$$\mathbf{y}(t) = \mathbf{W}\mathbf{x}(t), \tag{4}$$

where $\mathbf{y}(t) = (y_1(t), y_2(t), \ldots, y_m(t))^T$. Each separated output signal is presented as $y_i = w_i^T\mathbf{x}$ or $y = w^T\mathbf{x}$. With regards to the central limit theorem, maximizing the non-Gaussianity of y will make it to converge toward one of the ICs close to the original signals. The non-Gaussianity is measured by the negentropy function $J(y)$, expressed as

$$J(y) = H(y_{\text{Gauss}}) - H(y), \tag{5}$$

where y_{Gauss} is a Gaussian random variable having the same variance as that of the output signal y, and $H(y)$ the entropy of y. Hyvärinen[24] introduced an approximation of negentropy as

$$J(y) \approx \rho[E\{f(y)\} - E\{f(\nu)\}]^2, \tag{6}$$

where ρ is a positive constant that is set as one in our experiments, $f(\cdot)$ is a nonquadratic function, $E\{\cdot\}$ is an expectation operator and ν is a standard Gaussian variable with zero mean and unit variance. Usually, ICA identifies as many ICs as the number of observations, and an ordering of the extracted ICs is arbitrary.[25] Paradigm information has been used after ICA to select output components[26] but was not directly involved in the unmixing process of source signals.

2.2.2. *Constrained independent component analysis*

In this section, we describe the advantage of cICA to extract ICs of interest by defining constraints on the outputs of interest. Mathematically, the basics of cICA are formulated from the ICA algorithm with the main objective to maximize the negentropy term in Eq. (6). Apart from negentropy, additive constraints used to minimize the closeness measurement between the outputs and the references are presented by $g(y) = \varepsilon(y, r) - \xi \leq 0$ where ξ is the threshold, r the prior information guiding the output signals and $\varepsilon(y, r)$ the closeness measurement. The typical common form of $\varepsilon(y, r)$ used in our method is the mean square error (MSE) $\varepsilon(y, r) = E\{(y - r)^2\}$.

The optimization formulation of cICA is expressed by

$$\begin{array}{l} \text{maximize } J(y) = \rho(E\{f(y)\} - E\{f(\nu)\})^2 \\ \text{subject to } g(y) \leq 0 \end{array}, \tag{7}$$

or

$$\begin{array}{l} \text{minimize } \mathcal{J}(\mathbf{y} : \mathbf{W}) = -J(y) \\ \text{subject to } g(y) \leq 0 \end{array}, \tag{8}$$

where $\mathbf{W}$ is a demixing matrix. Assume that the Lagrange multiplier is μ, the optimization function is rewritten as

$$L(\mathbf{W}, \mu) = \mathcal{J}(\mathbf{y} : \mathbf{W}) + G(\mathbf{y} : \mathbf{W}, \mu). \tag{9}$$

The explicit form of $G(\mathbf{y} : \mathbf{W}, \mu)$ is found in Refs. 25 and 27. The Jacobian matrix of $L(\mathbf{W}, \mu)$ with respect to w is computed by $\nabla_w^2 L = (-E\{\hat{\rho} f''(y)\} + E\{\mu g_y''(y)\})\mathbf{\Sigma}_{xx}$ where $\hat{\rho} = 2\rho(E\{f(y)\} - E\{f(\nu)\})$ and $\mathbf{\Sigma}_{xx} = E\{\mathbf{x}\mathbf{x}^T\}$ is the covariance matrix.

The fast update rule for a one-unit reference derived by

$$\mu \leftarrow \max\{0, \mu + \gamma g(y)\},$$

$$w \leftarrow w - \nabla_w^2 L^{-1}(-E\{J'(y)\mathbf{x}^T\}^T + \mu\nabla_w g(y)^T),$$
$$w \leftarrow w/\|w\|, \tag{10}$$

where γ is the update rate. The parameters γ and ξ are fixed as 0.5 in all experiments. The update procedure described in Eq. (10) is repeated until the algorithm converges.[27–29] The reference signal is formed by a binary vector that gets the values of ones within an onset duration (stimulus is turned on) and zeros otherwise. The amplitude of the recovered IC will be estimated by the mixing and demixing matrix. Meanwhile, cICA is implemented by MATLAB 2008a. The cICA extraction procedure to acquire the true responses from the measurements using a reference is illustrated in Fig. 2.

2.3. *Evaluation metrics*

Contrast-to-noise ratio (CNR)[23] is used to reflect the differences between the signals during task and rest. The larger the CNR are, the better fNIRS signals are capable of presenting the actual changes of the brain activities.[30] An equation to compute CNR is expressed by

$$\text{CNR} = \frac{|\text{mean(task)} - \text{mean(rest)}|}{\text{var(task)} + \text{var(rest)}}, \tag{11}$$

where mean(task) and mean(rest) are the averages of the signals within the task duration and rest duration, respectively, var(task) and var(rest) are the standard variation of the signals within the two durations, and var(task) + var(rest) is used to normalize the values of CNR with regards to the variation of the signals.

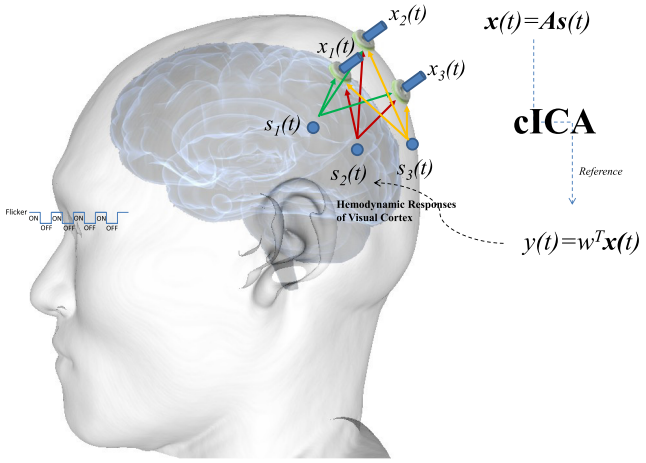

Fig. 2. Apply cICA to extract fNIRS signals from the mixtures.

3. Results

3.1. *Performance analysis of cICA*

We conducted both experiments with real data and simulations to validate the effects of cICA on task-related/nontask related signals as well as on visual/nonvisual signals at control regions. For experiments, only oxy-Hb signals were considered.

For simulations, we studied whether cICA may return false visual evoked responses from nontarget

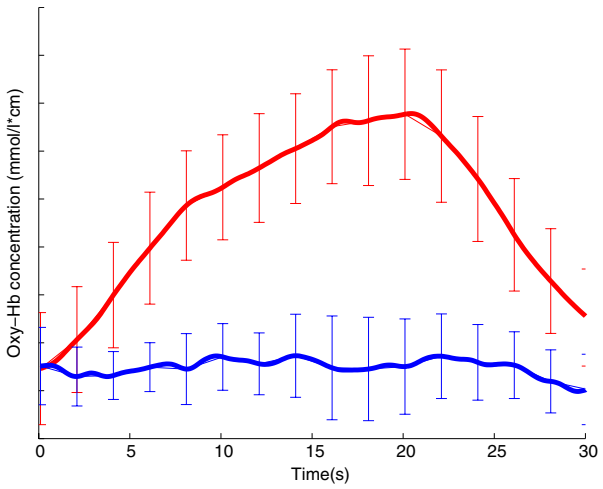

Fig. 3. Oxy-Hb concentration changes of the visual cortex corresponding to task (red curve) and nontask (blue curve) stimulus.

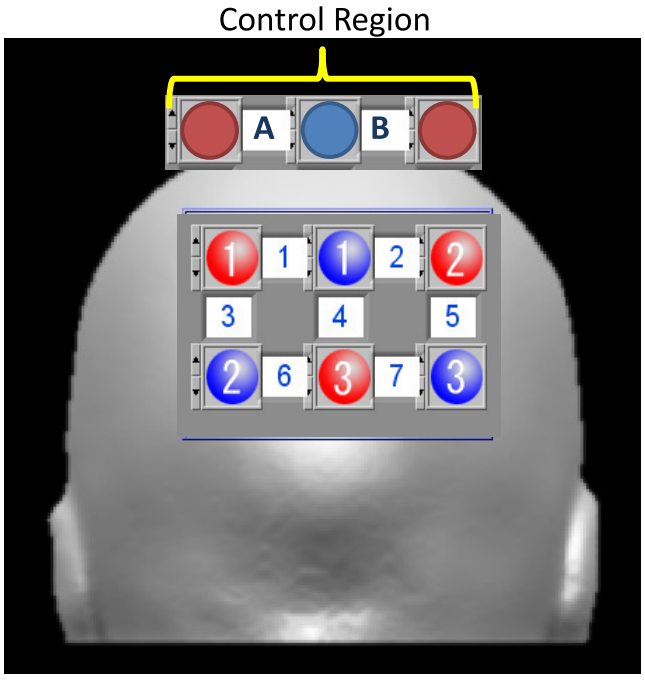

Fig. 4. Control region.

stimuli. We recorded 15-min data series (900 s) with a single subject. The subject is advised to take rest while the NIRS data were collected. Five synthetic oxy-Hb responses generated by a Gamma function[26] with the time constant of 3 s were randomly added into the data and separated by at least 60 s. We compared the components extracted by cICA between before and after the synthetic responses were added. The folding-average of the extracted components over five trials shown in Fig. 3 revealed that cICA has not returned a false task-related extraction.

Additionally, we designed a paradigm with real data to analyze the differences between signals extracted by visual at control regions. Four subjects were involved in this experiment. Configurations of probes to collect seven-channel data of visual cortex areas were presented in Sec. 2.1.3. Besides, we measured two extra channels **A** and **B** at control regions as illustrated in Fig. 4. Only two flickering

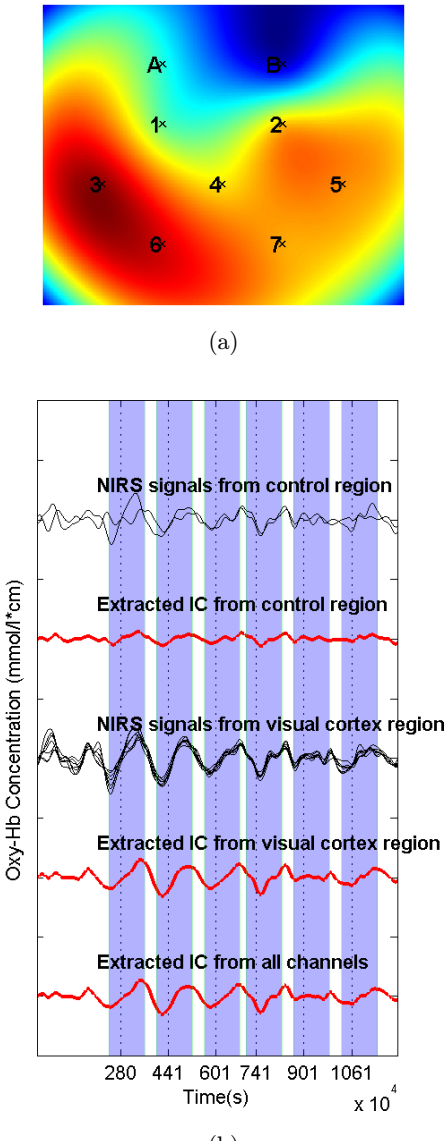

(a) (b)

Fig. 5. Evoked Oxy-Hb responses with 0 Hz flickering stimulus. (a) Spatial map of ICs extracted from all channels and (b) Extracted ICs and original signals of visual cortex region vs control region.

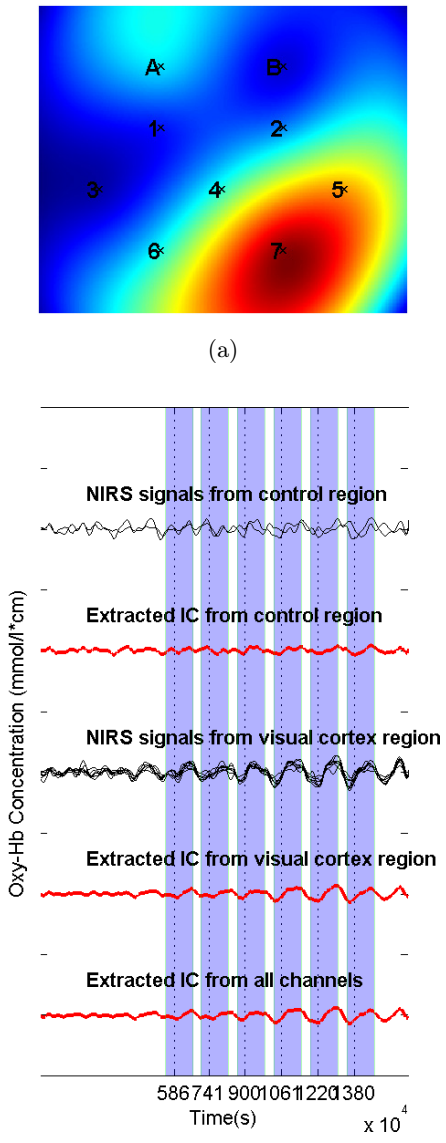

(a) (b)

Fig. 6. Evoked Oxy-Hb responses with 10 Hz flickering stimulus. (a) Spatial map of ICs extracted from all channels and (b) Extracted ICs and original signals of visual cortex region vs control region.

frequencies of 0 and 10 Hz have been examined to evoke hemodynamic responses of the brain. During experimental sessions, the visual flickering was randomly turned on and lasted for 60 s. The trials were repeated for six times. Recovered oxy-Hb and deoxy-Hb ICs of one participant by applying cICA on all measured channels including channels of visual cortex and channels of control regions are shown in Figs. 5 and 6. When all channels were used, corresponding spatial map of the extracted components were described to show that active regions belong to the visual cortex of the brain. Average CNR values in comparing hemodynamic responses between 20 s before and 60 s after a stimulus occurred were reported: CNR values of recovered oxy-Hb signals between visual and control regions are 0.81 and 0.43 for 0 Hz flickering stimulus and 0.58 and 0.21 for 10 Hz flickering stimulus. We see that cICA performed better in terms of CNR on the visual cortex region where the recovered hemodynamic responses were associated with the target stimuli.

3.2. *Hemodynamic responses within task and rest duration*

Before considering the hemodynamic changes with regards to the modulation depth and flickering frequency of lights, we examined how the visual cortex acts with and without the presence of visual stimulus. We applied t-test and CNR to validate the responses of the oxy-Hb and deoxy-Hb concentration within the task and the rest duration. To evaluate the efficiency of utilizing cICA in extracting the actual responses of fNIRS on a block experiment, we compared the results of cICA with CBSI[23] applied on the fNIRS signals.

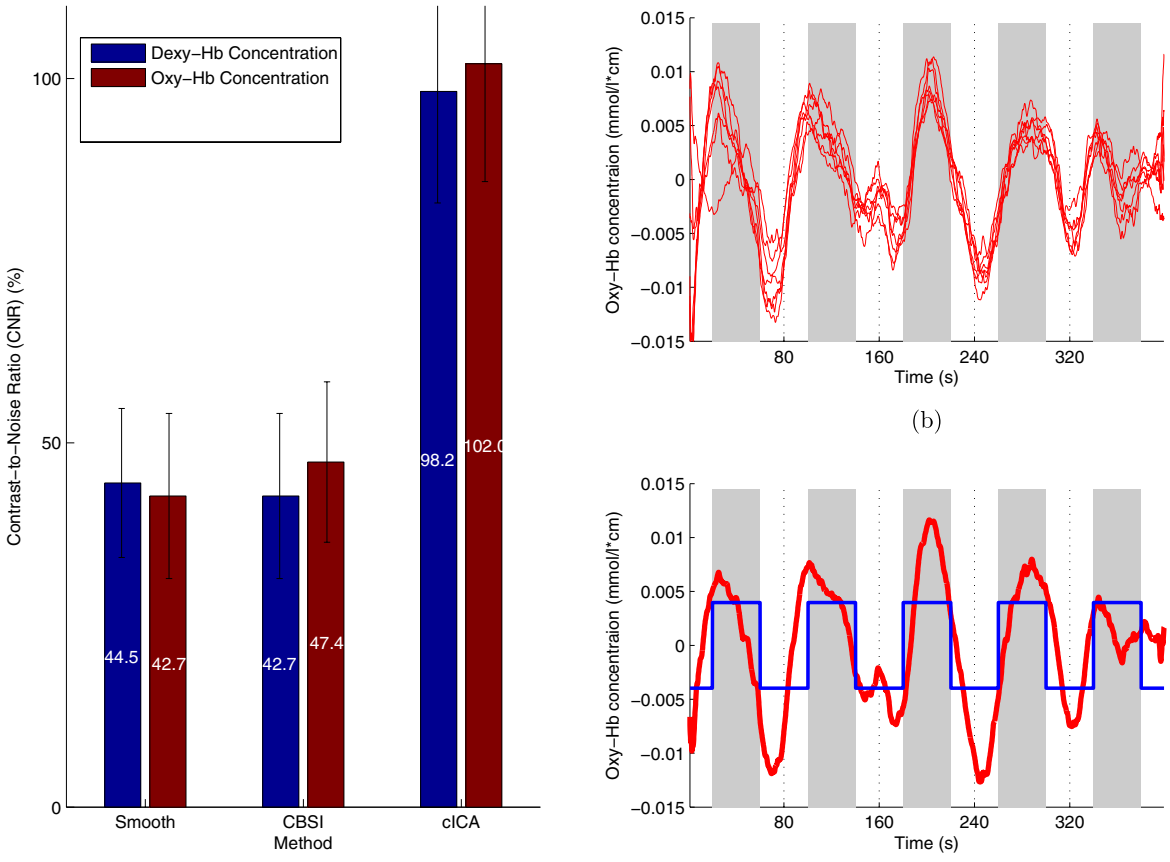

Fig. 7. Improved fNIRS signals using cICA. (a) CNR Comparison of hemoglobin concentration between rest and task of raw fNIRS signals (only smoothing is utilized), fNIRS signals improved by CBSI and cICA, respectively, (b) an example of oxy-Hb concentration signals over 7 channels, and (c) an example of oxy-Hb concentration signal extracted from those mixtures by cICA.

Paired-sample t-test analysis showed that even when there were no improvement (only smoothing was used), the differences of hemodynamic responses between task and rest duration were significant for both oxy-Hb concentration and deoxy-Hb concentration ($p < 0.0001$) revealing the fNIRS responses to the visual stimulation. When CBSI and cICA were used, the oxy-Hb and deoxy-Hb concentrations between task and rest remained significantly different ($p < 0.0001$). However, the responses of fNIRS within the onset duration became larger when cICA and CBSI were applied and cICA achieved the best results in comparison with other techniques in terms of CNR as illustrated in Fig. 7(a).

The folding-average of the oxy-Hb and deoxy-Hb concentration over all frequencies, modulations and subjects are summarized in Fig. 8. The results well reflect typical hemoglobin responses with the increasing of oxy-Hb and decreasing of deoxy-Hb during onset periods.

3.3. *Human flickering sensitivity to various modulation depths and frequencies of stimuli*

3.3.1. *fNIRS responses to different frequencies of flickering light*

Previous studies[16] found that when the subjects were watching several spatial and temporal visual patterns, the hemodynamic responses of the visual cortex showed no significant differences. In our experiment, we investigated the visual cortex responses to four stimulus temporal frequencies of 0, 5, 10 and 15 Hz. The ANOVA analysis among

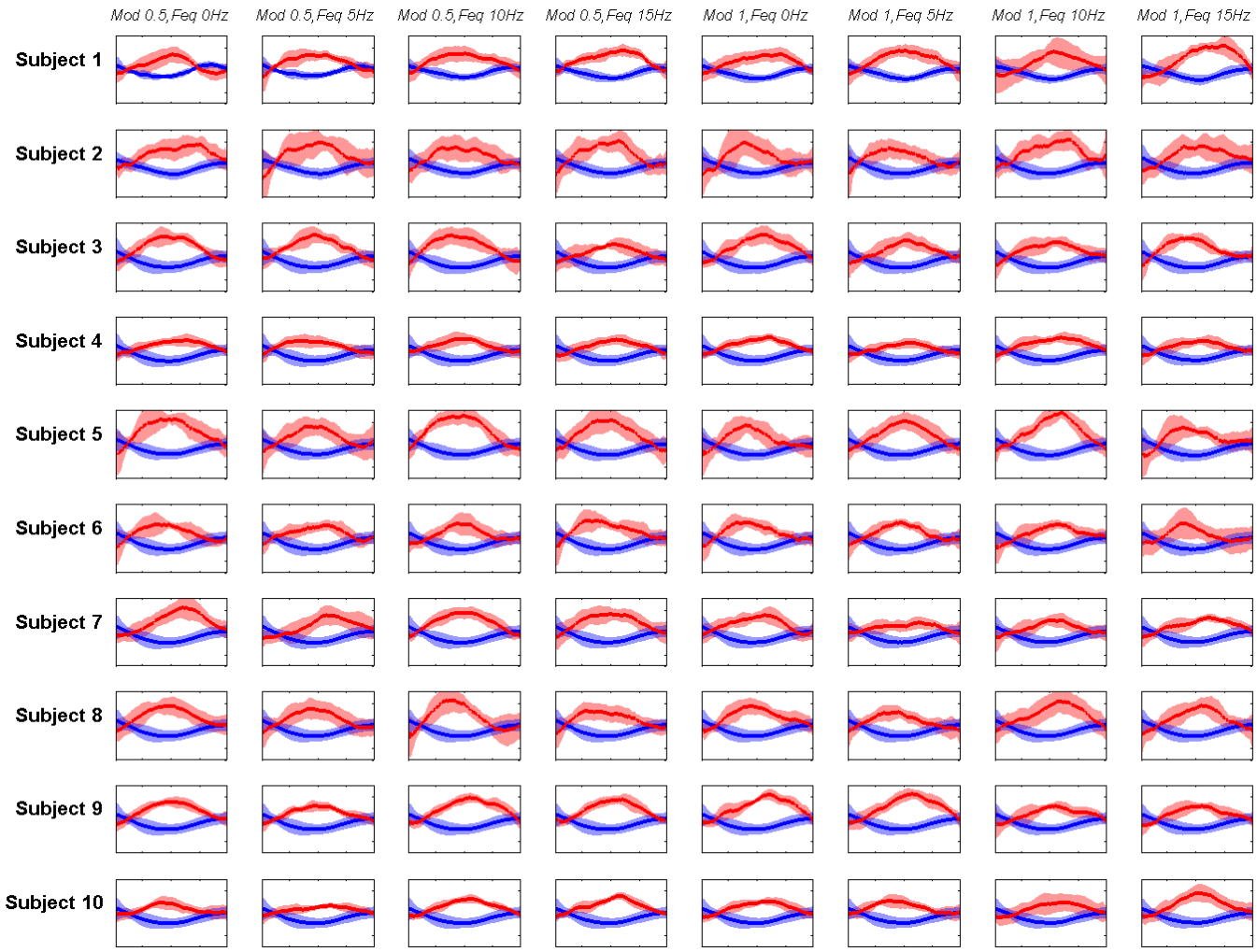

Fig. 8. The folding-average of the oxy-Hb and deoxy-Hb concentration over all frequencies, modulations and subjects. Oxy-Hb curves are in red while deoxy-Hb curves are in blue.

four groups revealed no significant separation on oxy-Hb concentrations ($F(3, 796) = 1.387, p < 0.246$) and deoxy-Hb concentrations ($F(3, 796) = 1.201$, $p < 0.308$). Taking an average of the fNIRS signals over five epochs for each experimental session, ANOVA test also inferred no significant changes of oxy-Hb concentration ($F(3, 156) = 1.182, p < 0.319$) and of deoxy-Hb concentration ($F(3, 156) = 0.765, p < 0.515$) on various frequencies.

3.3.2. *fNIRS responses to different modulation depths of flickering light*

In this experiment, two stimulus modulation depths of 0.5 and 1.0 were used. A small change of oxy-Hb concentrations was observed. However, sample t-test showed that the change was not significant ($p < 0.234$, $df = 798$, $t = 1.191$). Similarly, the modulation inclines led to the upward trends of the deoxy-Hb concentration, but the changes were miniscule ($p < 0.277$, $df = 798$, $t = -1.087$). We acquired the same results on the means of the oxy-Hb and deoxy-Hb concentration over the five trials of each session: The results from the t-test suggested that alternations found on mean oxy-Hb responses and mean deoxy-Hb responses were not statistically significant ($p < 0.273$, $df = 158$, $t = 1.099$) and ($p < 0.386$, $df = 158$, $t = -0.869$). Figure 9 illustrates the average hemodynamic responses between the two modulations depths. Marginally, oxy-Hb concentration tended to decrease (8 over 10 subjects) and deoxy-Hb concentration tended to increase when a lower modulation of flickering stimulus was present.

3.3.3. *Interaction of modulation and frequency of flickering stimuli to hemodynamic responses of visual cortex*

Factorial 2×4 ANOVA were used to analyze the interaction of the two modulation depths and four flickering frequencies. The main effect reported no interaction between modulation levels and frequencies for oxy-Hb concentration ($F = 0.378, p < 0.769$) and for deoxy-Hb concentration ($F = 1.231$, $p < 0.297$). The estimated marginal means of oxy-Hb and deoxy-Hb concentration are depicted in Fig. 10. We found that oxy-Hb concentration of the

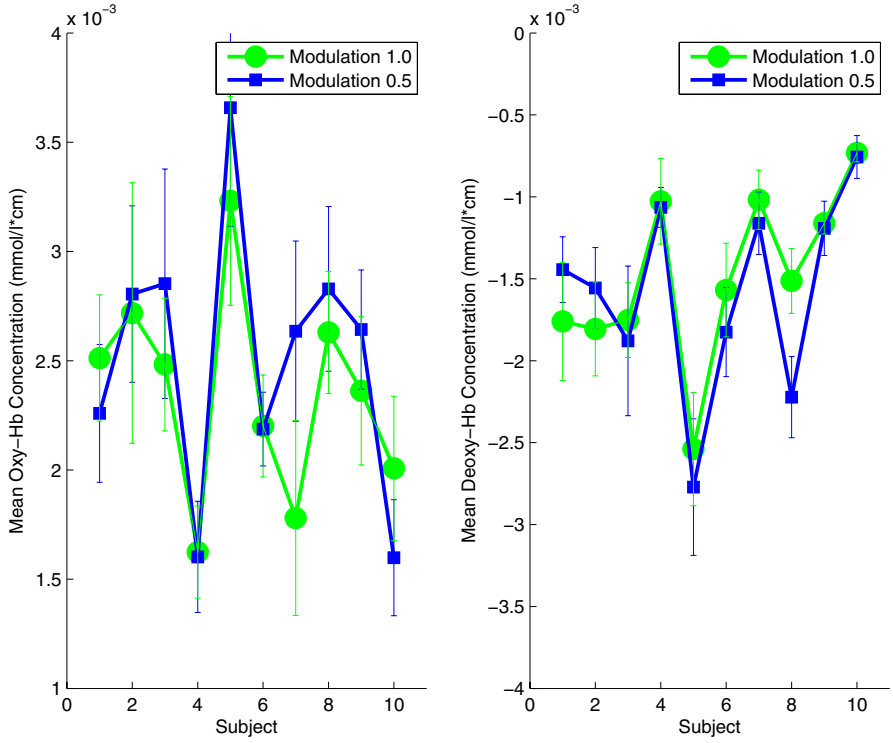

(a) (b)

Fig. 9. Hemodynamic responses of the visual cortex to the two modulations depths of the flickering stimuli. (a) Oxy-Hb concentration and (b) Deoxy-Hb concentration.

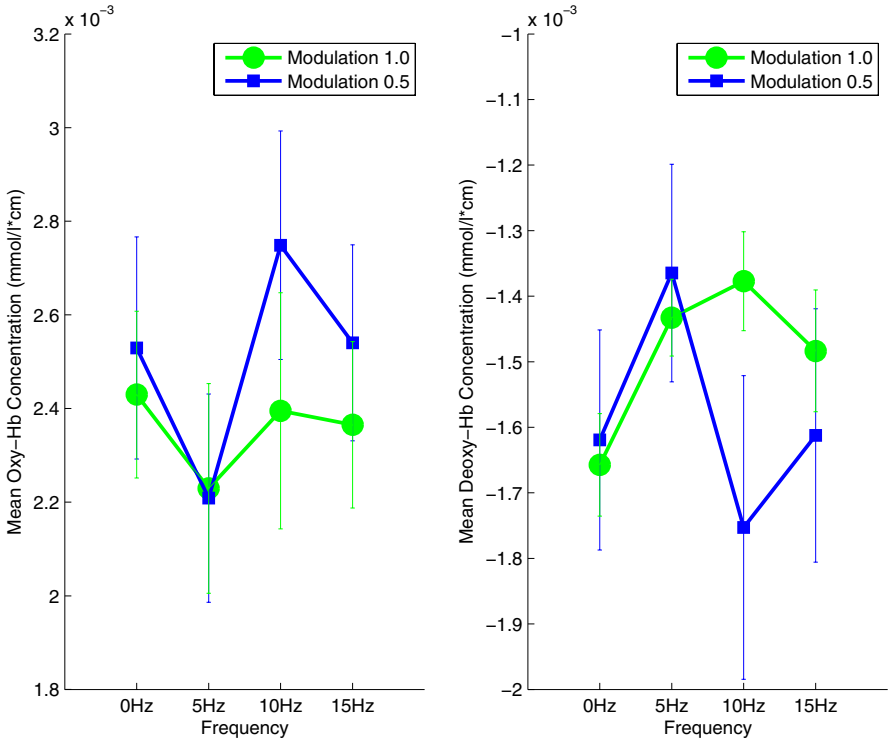

Fig. 10. Interaction of the modulation and frequency of flicking stimuli. (a) Oxy-Hb concentration and (b) Deoxy-Hb concentration.

modulation 0.5 was higher than that of the modulation 1 with an average increase percentage of 5.69%. At the frequency of 10 Hz, the decrease of deoxy-Hb in terms of modulation was significant ($p < 0.03, df = 198, t = -2.179$).

4. Conclusions and Discussion

This study investigated the hemodynamic responses of the visual cortex of 10 healthy subjects while stimulating their eyes with a light beam modulated sinusoidally. Frequencies were varied in the range of 0 to 15 Hz and the modulation depth in the range of 0.5 to 1. To enhance the quality of the desired fNIRS signals, we used cICA to improve actual NIRS responses from the obtained event-related fNIRS measurements. The prior information integrated in cICA regulated the estimated ICs toward paradigm information. Experimental results have showed that the proposed method was effective to acquire task-related components from the NIRS mixtures: with the help of cICA, CNR reflecting the contrast of hemodynamic concentration between rest and task became larger, showing improvements of cICA when the noises were present in the NIRS signals.

The experiments to determine the variations of the mean values of oxy-Hb and deoxy-Hb concentration within the task duration revealed significant changes of the hemodynamic responses of the visual cortex from the baseline when the flickering stimulation was activated. In subsequent studies, we found that there was slight decrease of the oxygenated hemoglobin concentration over four frequencies when the modulation increased. However, the variations of oxy and deoxy-hemoglobin over different stimulus conditions were not statistically significant.

It is unclear why we obtained such a weak correlation between photic sinusoidal stimulation and the oxy-Hb and deoxy-Hb changes. In the physiological aspect, such a stimulation induces clear neuronal responses using measurement methods such as psychophysics, electrophysiology and fMRI. The fNIRS is a powerful method to monitor hemodynamic responses of the brain but may not be appropriate to monitor deep neural layers to find coupling between neural responses and oxy-Hb and

deoxy-Hb concentrations. Bridge[16] used pattern stimulation in combination with temporal stimulation and also found insignificant differences of the brain responses to various temporal frequencies of stimuli. He also suggested that it may be due to fNIRS limitations. The issue of weak correlation between photic sinusoidal stimulation and the oxy-Hb and deoxy-Hb changes is still open for discussion and further investigations.

Acknowledgments

This research was supported by Vietnam National University-Ho Chi Minh City research grant B2011-28-01.

References

1. P. M. Roget, "Explanation of an optical deception in the appearance of the spokes of a wheel seen through vertical apertures," *Philis. Trans. R. Soc. Lond.* **115**, 131–140 (1825).
2. S. Hecht, S. Shlaer, "Intermittent stimulation by light: V. The relation between intensity and critical frequency for different parts of the spectrum," *J. Gen. Physiol.* **19**, 965–979 (1936).
3. S. L. Machnik, "Visual masking approaches to visual awareness," *Prog. Brain Res.* **155**, 177–215 (2006).
4. V. V. Toi, C. W. Burckhardt, P. A. Grounauer, "Irregularities in the flicker sensitivity curve," *Appl. Opt.* **30**, 2113–2120 (1991).
5. H. De Lange, "Research into the dynamic nature of the human fovea-cortex system with intermittent and modulated light," *J. Opt. Soc. Am.* **48**, 777–784 (1958).
6. C. Sternheim, C. Cavonius, "Sensitivities of the human ERG and VECP to sinusoidally modulated light," *Vision Res.* **12**, 1685–1695 (1972).
7. V. V. Toi, C. Riva, "Variations of blood flow at optic nerve head induced by sinusoidal flicker stimulation in cats," *J. Physiol. (London)* **482**, 189–202 (1995).
8. B. Cleland, C. Enroth-Cugell, "Cat retinal ganglion cell responses to changing light intensities: Sinusoidal modulation in the time domain," *Acta Physiol. Scand.* **68**, 365–381 (1966).
9. C. Kaufmann, G. K. Elbel, C. Goessl, B. Puetz, D. P. Auer, "Frequency dependence and gender effects in cortical visual processing observed with fMRI using a temporally graded dartboard stimulus," *Hum. Brain Imaging* **14**, 28–38 (2001).
10. B. Ozus, H. Liu, L. Chen, M. B. Iyer, P. T. Fox, J. Gao, "Rate dependence of human visual cortical response due to brief stimulation: An event-related FMRI study," *Magn. Reson. Imaging.* **19**, 21–25 (2001).
11. M. A. McIntosh, U. Shahani, R. G. Boulton, D. L. McCulloch, "Absolute quantification of oxygenated hemoglobin within the visual cortex with functional near infrared spectroscopy (fNIRS)," *Invest. Ophthalmol. Vis. Sci.* **51**, 4856–4860 (2010).
12. J. H. Meek, C. E. Elwell, M. J. Khan, "Regional changes in cerebral haemodynamics as a result of a visual stimulus measured by near infrared spectroscopy," *Proc. R. Soc. B Biol. Sci.* **261**, 351–356 (1995).
13. H. Kojima, T. Suzuki, "Hemodynamic change in occipital lobe during visual search: Visual attention allocation measured with NIRS," *Neuropsychologia* **48**, 349–352 (2010).
14. S. Wijeakumar, U. Shahani, W. A. Simpson, D. L. McCulloch, "Localization of hemodynamic responses to simple visual stimulation: An fNIRS study," *Invest. Ophthalmol. Vis. Sci.* **53**, 2266–2273 (2012).
15. S. M. Liao, N. M. Gregg, B. R. White, B. W. Zeff, K. A. Bjerkaas, T. E. Inder, J. P. Culver, "Neonatal hemodynamic response to visual cortex activity: High-density near-infrared spectroscopy study," *J. Biomed. Opt.* **15**, 026010 (2010).
16. T. Bridge, "Measuring the haemodynamic responses elicited in the visual cortex from various spatial and temporal frequencies using NIRS," *The Plymouth Student Scientist.* **5**, 94–118 (2012).
17. V. V. Toi, P. A. Grounauer, "Visual stimulator," *Rev. Sci. Instrum.* **49**, 1403–1406 (1978).
18. V. D. Calhoun, T. Adali, M. C. Stevens, K. A. Kiehl, J. J. Pekar, "Semi-blind ICA for fMRI: A method for utilizing hypothesis-derived time courses in a spatial ICA analysis," *NeuroImage* **25**, 527–538 (2005).
19. C. Guignard, V. V. Toi, C. W. Burckhardt, J. L. Schelling, "Sensitivity to the flickering light in digitized patients," *Br. J. Clin. Pharmacol.* **15**, 189–196 (1983).
20. V. V. Toi, C. W. Burckhardt, P. A. Grounauer, "Flicker-fusion perception investigations: Design, modeling and applications," *International J. Precision Mach. Med. Eng. Mecha-Optoelectron.* **1**, 355–376 (1987).
21. V. V. Toi, "Derivation of a unified transfer function in the theory of flicker," *Opt. Lett.* **14**, 907–909 (1989).
22. T. Li, H. Gong, Q. Luo, "Visualization of light propagation in visible Chinese Human head for functional near-infrared spectroscopy," *J. Biomed. Opt.* **16**, 045001 (2011).
23. X. Cui, S. Bray, A. Reiss, "Functional near infrared spectroscopy (NIRS) signal improvement based on

negative correlation between oxygenated and deoxygenated hemoglobin dynamics," *NeuroImage* **49**, 3039–3046 (2010).
24. A. Hyvärinen, J. Karhunen, E. Oja, "*Independent Component Analysis*," John Wiley and Sons (2001).
25. W. Lu, J. C. Rajapakse, "Approach and applications of constrained ICA," *IEEE Trans. Neural Netw.* **1**, 203–212 (2005).
26. C. B. Akgul, A. Akin, B. Sankur, "Extraction of cognitive activity-related waveforms from functional near-infrared spectroscopy," *Med. Biol. Eng. Comput.* **44**, 945–958 (2006).
27. N. D. Thang, T. Rasheeda, Y.-K. Lee, S. Lee, T.-S. Kim, "Content-based facial image retrieval using constrained independent component analysis," *Inform. Sci.* **181**, 3162–3174 (2011).
28. Z.-L. Sun, L. Shang, "An improved constrained ICA with reference based unmixing matrix initialization," *Neurocomputing* **73**, 1013–1017 (2010).
29. Z. Wang, "Fixed-point algorithms for constrained ICA and their applications in fMRI data analysis," *Magn. Reson. Imaging.* **29**, 1288–1303 (2011).
30. Q. Zang, G. E. Strangman, G. Ganis, "Adaptive filtering to reduce global interference in non-invasive NIRS measures of brain activation: How well and when does it work?," *NeuroImage* **25**, 527–538 (2005).